Stability Assessment using Adaptive Interval Type-2 Fuzzy Sliding Mode Controlled Power System Stabilizer

Dipak R Swain
OUTR Bhubaneswar
PRAKASH K RAY
OUTR Bhubaneswar
Ranjan K Jena
OUTR Bhubaneswar
SHIBA R PAITAL (shiba.paital@gmail.com)
OUTR Bhubaneswar https://orcid.org/0000-0002-3883-0144

Research Article

Keywords: Adaptive Interval type-2 fuzzy sliding mode control (AIT2FSMC), Low frequency electromechanical oscillations (LFEOs), PSS, MMPS, SMIB

Posted Date: June 22nd, 2022

DOI: https://doi.org/10.21203/rs.3.rs-1412744/v1

Stability Assessment using Adaptive Interval Type-2 Fuzzy Sliding Mode Controlled Power System Stabilizer

Dipak R. Swain[1], Prakash K. Ray[1], Ranjan K. Jena[1], Shiba R. Paital[1*]

[1] Department of Electrical Engineering, OUTR Bhubaneswar, Odisha, India
Corresponding Author-[*]shiba.paital@gmail.com

Abstract: The low frequency electromechanical oscillations (LFEOs) in electric power system are because of weaker inter-ties, uncertainties, various faults and disturbances. These LFEOs (0.2-3 Hz.) are less in magnitude and are responsible for lower power transfer, increased losses and also threaten the stability of power system. An adaptive interval type-2 fuzzy sliding mode controlled power system stabilizer (AIT2FSMC-PSS) is presented to neutralize the LFEOs and enhance stability under uncertainties and external disturbances. The AIT2FSMC is a hybridization of type-2 fuzzy logic system (T2FLS) with conventional SMC to lower the chattering effect, enhance the robustness of reaching phase and improve system's performance. Here, T2FLS is used for estimating the unknown functions of SMC. A robust sliding surface is presented to keep the system in the desired plane and remain stable under disturbance conditions. A modified control law is proposed for selecting the control parameters and Lyapunov synthesis is used to make the error asymptotically converging to zero. The effectiveness of the AIT2FSMC-PSS is accessed in single and multimachine power systems subjected to various uncertainties and disturbances. Again, comparison of performance indices (PIs), Eigen values, damping ratios, oscillating frequencies, integral time absolute error (ITAE), figure of demerit (FD) and frequency domain plots like Bode, root locus and Nyquist plots are also analyzed to access the efficacy of the proposed stabilizer. The simulated responses, comparative study and frequency plots conform the supremacy of the proposed AIT2FSMC-PSS in suppressing the LFEOs with lesser settling characteristics, offer stable performance and assures transient stability of power system as compared to other stabilizers.

Keywords: Adaptive Interval type-2 fuzzy sliding mode control (AIT2FSMC), Low frequency electromechanical oscillations (LFEOs), PSS, MMPS, SMIB.

1. Research Background

Modern power systems are complex and extremely nonlinear in nature. They operate at increased stress and sometimes near their stability limits to ensure continuity of power supply. Disturbances such as faults, load perturbations, natural disasters etc. are responsible for the generation of LFEOs in the range of (0.2-3) Hz [1]. LFEOs are small in magnitude but sustain for long durations and results in degraded power transfer, loss of synchronism, subsequent blackouts and power outages [2]. LFEOs are classified into local and interarea mode of oscillations. Oscillations in local generators located in one geographical area are local oscillations (0.8-3) Hz. whereas, oscillations in generators located in different areas are called interarea mode oscillations (0.1-0.7) Hz. Among which, interarea oscillations should be handled more cautiously than local oscillations because it can lead to generation failure [3]-[4]. Stability of power system depend on the operating conditions. Out of different classes of stability, transient stability is at higher priority because it is related to maintaining synchronism between the generators under severe disturbance conditions.

Conventionally, oscillation damping is achieved through fast acting high gain excitation systems. But, it produces negative damping torques in the power system [5]. In past decades, lead-lag based PSS are adopted to provide stabilizing signals to the exciter for damping the LFEOs. It has predefined parameters and provides good damping characteristics in a linearized model of power system. But, due to fixed parameters of PSS, its performance degrades under change in operating point which results in oscillatory instability [6]. Hence, to overcome the limitations of CPSS, several compositions of PSS like H-infinity [7], pole placement [8], LMI method [9], proportional integral derivative (PID) [10], and fractional order PID (FOPID) [11] has been proposed in literatures. For improved performance, various nature inspired optimization mentioned in the literatures [12]-[17] are used for optimizing the parameters of PSS.

In addition to the existing control approaches, fuzzy logic control (FLC) has been extensively used for the design of PSS as reported in literatures [18]-[20]. Being a nonlinear control technique, FLC based PSS (FPSS) provide good oscillation damping performance to that of CPSS. It is applicable to problems where mathematical model is not available. But, its performance gets degraded while handling nonlinearities and uncertainties. Hence, to overcome this limitation, adaptive control strategy based FLC is introduced [21]-[22]. But, it cannot offer the required oscillation damping characteristics under severe disturbances. Nowadays, a robust control technique called sliding mode control (SMC) was gaining popularity because of its simplest structure, superior disturbance elimination and insensitive to parameter variations [23]. But, it has its own limitations such as (i) it requires proper knowledge of system dynamics (ii) chattering phenomenon due to discontinuous control law. SMC performs efficiently under normal operating conditions. But its performance gets degraded under large and continuously varying disturbance conditions. To overcome the above said limitations, SMC is hybridized with FLC to ameliorate the system performance [24]. However, oscillations are still present under transient disturbance conditions. Hence, different higher order SMC is adopted in literature [25]-[28]. In this regard, an AFSMC based PSS without reaching phase is presented in [25] for damping out LFEOs under disturbance conditions. An indirect AFSMC-PSS is suggested by Saoudi et al. for minimizing oscillations in multimachine power system [26]. Again, an AFSMC-PSS is suggested in [27] for improving stability in SMIB and MMPS and also validated their approach in a real time simulator. An AFSMC with PI surface is proposed in [28] to damp out oscillations and enhancing stability. Although, the above said methods are based on type-1 FLC (T1FLC) which has limitations in dealing with large uncertainties and unexpected disturbances in the power system. Hence, an extension of T1FLC called type-2 FLC has been introduced. It has been applied in many real time applications, industrial control applications etc. T2FLC can easily handle the uncertainty factors more effectively because of its particular structure of its membership functions (MFs) [29].

Many applications of T2FLC for improvement of power system stability can be found in literature [30]-[34]. Shokouhandeh and Jazaeri have applied a robust T2FLC based PSS for handling uncertainties due to loading and line parameters [30]. Sambariya et al. have implemented IT2FPSS enhancing stability in single and MMPS subjected to disturbances [31]. Sun et al. presented a differential evolution (DE) tuned T2FLC based PSS for stability improvement of power system [32]. A hybrid firefly swarm algorithm tuned IT2FOFPID-PSS is suggested in [33] for enhancing stability in both single and MMPS subjected to disturbances and uncertainties. Again, application of T2FLC based SMC can be found in [35]-[36]. Nechadi et al. proposed a T2AFSMC based PSS without reaching phase for damping oscillations of power system under disturbances [36].

Comparing the previously published papers, the following contributions are made and are presented as follows:

1. An AIT2FSMC based PSS is presented for damping of LFEOs under various power system uncertainties like noise and external disturbances.

2. IT2FLC is used for estimating the unknown functions and a modified control law is presented to avoid chattering effect. Lyapunov stability criteria is used for assuring stability such that the error asymptotically converges to zero.
3. Speed deviation ($\Delta\omega$) and accelerating power (ΔP) are considered as input signals. The effectiveness and efficacy of AIT2FSMC-PSS is accessed in single and 2-area, 16-machine, 68 bus power system under uncertainties and disturbances.
4. Comparison of PIs like settling time, overshoots, Eigen values, damping ratios, oscillating frequencies, ITAE, FD and frequency plots like Bode, root locus and Nyquist plots are provided to access the stability.
5. The simulated responses, comparative study and frequency plots conform the supremacy of the proposed AIT2FSMC-PSS in minimizing LFEOs with lesser peak and settling characteristics and offer more stable performance and assures transient stability to that of AFSMC-PSS, FSMC-PSS, FPSS and CPSS.

The paper is arranged as follows: the modelling of the power system is given in section-2. Introduction to AIT2FSMC is presented in section-3. Section-4 presents the simulations and the comparative analysis. Section-6 gives the concluding remarks and future scope followed by references.

2. Power System Modelling

The stability analysis is performed through modelling of different power system components. The dynamics of various components are framed using algebraic equations. The dynamics of multimachine power system is characterized by an i^{th} synchronous generator, exciter and other components. These equations are formulated by assuming fixed input mechanical power under disturbance conditions. The expressions representing the rotor dynamics of generator-i are given by [37].

$$\frac{d\delta_i}{dt} = \omega_i - \omega_s \tag{1}$$

Where, $\delta_i, \omega_i, \omega_s$ denote rotor angle, synchronous speed and base speed.

The change in rotor angle of i^{th} generator in terms of swing equation is given by:

$$\frac{2H}{\omega_s} \cdot \frac{d^2\delta}{dt^2} = T_{mi} - T_{ei} \tag{2}$$

Where, H, T_m, T_e are called inertia, mechanical and electrical torques. The electrical torque of i^{th} generator is calculated from the sub transient model. Hence, Eq. (2) can be rewritten as:

$$\frac{d\omega_i}{dt} = \frac{\omega_s}{2H}\left[\begin{array}{l} T_{mi} - D(\omega_i - \omega_s) - \frac{(X''_{di} - X_{lsi})}{(X'_{di} - X_{lsi})} E'_{qi} I_{qi} - \frac{(X'_{di} - X''_{di})}{(X'_{di} - X_{lsi})} \psi_{1di} I_{qi} - \frac{(X''_{qi} - X_{lsi})}{(X'_{qi} - X_{lsi})} E'_{di} I_{di} \frac{(X'_{qi} - X''_{qi})}{(X'_{qi} - X_{lsi})} \psi_{2qi} I_{di} \\ +(X''_{qi} - X''_{di}) I_{qi} I_{di} \end{array}\right] \tag{3}$$

Where, I_{di}, I_{qi} denote the stator currents in d and q-axis, ψ_{1di}, ψ_{2qi} represent d and q-axis transient and sub-transient EMFs, $X_{di}, X'_{di}, X''_{di}$ and $X_{qi}, X'_{qi}, X''_{qi}$ represent synchronous, transient and sub-transient reactances in d and q-axis. X_{lsi} is the leakage reactance of armature.

The expression of transient EMFs are as follows:

$$\frac{dE'_{qi}}{dt} = \frac{1}{T'_{doi}}\left[-E'_{qi} - (X_{di} - X'_{di})\left\{ -I_{di} - \frac{(X'_{di} - X_{di})}{(X'_{di} - X_{lsi})^2}\left(\psi_{1di} - (X'_{di} - X_{lsi}) I_{di} - E'_{qi}\right)\right\} + E_{fdi} \right] \tag{4}$$

$$\frac{dE'_{di}}{dt} = \frac{1}{T'_{qoi}}\left[-E'_{di} - (X_{qi} - X'_{qi})\left\{ -I_{qi} - \frac{(X'_{qi} - X''_{qi})}{(X'_{qi} - X_{lsi})^2}\left(-\psi_{2qi} + (X'_{qi} - X_{lsi}) I_{qi} - E'_{di}\right)\right\}\right] \tag{5}$$

Where, T'_{doi}, T'_{qoi} denote transient time constants in d and q-axis. E'_{di}, E'_{qi} represent transient voltage in d and q-axis, E_{fdi} is the field voltage of d-axis.

The expression for transient and sub-transient EMFs are as follows:

$$\frac{d\psi_{1di}}{dt} = \frac{1}{T''_{d0i}}\left[-\psi_{1di} + E'_{qi} + \left(X'_{di} - X_{lsi}\right)I_{di}\right] \tag{6}$$

$$\frac{d\psi_{2qi}}{dt} = -\frac{1}{T''_{q0}}\left[\psi_{2qi} + E'_{di} - \left(X'_{qi} - X_{lsi}\right)I_{qi}\right] \tag{7}$$

The expressions representing stator dynamics of generator-i are as follows:

$$V_i \cos\left(\delta_i - \theta_i\right) - \frac{\left(X''_{di} - X_{lsi}\right)}{\left(X'_{di} - X_{lsi}\right)}E'_{qi} - \frac{\left(X'_{di} - X''_{di}\right)}{\left(X'_{di} - X_{lsi}\right)}\psi_{1di} + R_{si}I_{qi} - X''_{di}I_{di} = 0 \tag{8}$$

$$V_i \sin\left(\delta_i - \theta_i\right) - \frac{\left(X''_{qi} - X_{lsi}\right)}{\left(X'_{qi} - X_{lsi}\right)}E'_{di} - \frac{\left(X'_{qi} - X''_{qi}\right)}{\left(X'_{qi} - X_{lsi}\right)}\psi_{2qi} + R_{si}I_{di} - X''_{qi}I_{di} = 0 \tag{9}$$

Where, V_i, R_{si} denote terminal voltage and armature resistance of i^{th} synchronous generator.

The saturation function of exciter is given by:

$$S_E\left(E_{fd}\right) = A_s e^{B_s E_{fd}} \tag{10}$$

Where, A_s, B_s are the saturation constants.

The algebraic equations representing the dynamics of excitation system are as follows:

$$\frac{dV_{tri}}{dt} = \frac{1}{T_{ri}}\left[-V_{tri} + V_{ti}\right] \tag{11}$$

$$\frac{dE_{fdi}}{dt} = -\frac{1}{T_{Ei}}\left[K_{Ei}E_{fdi} + E_{fdi}A_{ex}e^{B_{ex}E_{fdi}} - V_{ri}\right] \tag{12}$$

$$\frac{dV_{ri}}{dt} = \frac{1}{T_{Ai}}\left[\frac{K_{Ai}K_{Fi}}{T_{Fi}}R_{Fi} + K_{Ai}\left(V_{refi} - V_{tri}\right) - \frac{K_{Ai}K_{Fi}}{T_{Fi}}E_{fdi} - V_{ri}\right] \tag{13}$$

$$\frac{dR_{Fi}}{dt} = \frac{1}{T_{Fi}}\left[-R_{Fi} + E_{fdi}\right] \tag{14}$$

Where, V_{tri}, V_{ti} represent measured voltage state variable and terminal voltage.

The expression of i^{th} PSS is given as:

$$V_{PSSi} = K_{PSSi}\left[\frac{sT_w}{1 + sT_w}\right]\left[\frac{1 + sT_{1i}}{1 + sT_{2i}}\frac{1 + sT_{3i}}{1 + sT_{4i}}\right] \tag{15}$$

Where, $T_w, T_{1i}, T_{2i}, T_{3i}, T_{4i}$ denote washout and lead-lag time constants.

3. Adaptive Interval Type-2 Fuzzy Sliding Mode Control (AIT2FSMC)

3.1. Type-2 Fuzzy Logic Systems (T2FLS)

T2FLS are the extension of T1FS. It was presented by Lotfi Zedeh in 1975 and then developed by Karnik and Mendel in 1999 [38]. It uses the concept of fuzzy sets for handling uncertainties, nonlinearities and unexpected disturbances. The T1FLS has a two dimensional MF representing crisp values [0,1] whereas T2FLS have a 3D membership function. A T2FS denoted by $\tilde{A}$ is expressed as $0 \le \mu_{\tilde{A}}\left(x,u\right) \le 1$, $\forall x \in X$, $\forall u \in J_x \subset \left[0,1\right]$ which consisting of upper MF (UMF) $\bar{\mu}_{\tilde{A}}\left(x\right)$ and lower MF (LMF) $\underline{\mu}_{\tilde{A}}\left(x\right)$ separated by a footprint of uncertainty (FOU) as shown in Fig. 1 (a). When $\mu_{\tilde{A}}\left(x,u\right) = 1$, $\forall u \in J_x \subset \left[0,1\right]$ then, iy is called as an interval type-2 MF and also called IT2FSs.

The control diagram of T2FLC is given in Fig. 1 (b). The functioning of each blocks are described as follows [33], [39].

1. Fuzzifier

Fuzzifier converts crisp values $(e_1, e_2....e_n)^T$ into IT2FS $\tilde{A}_x$. A singleton type fuzzifier is adopted here.

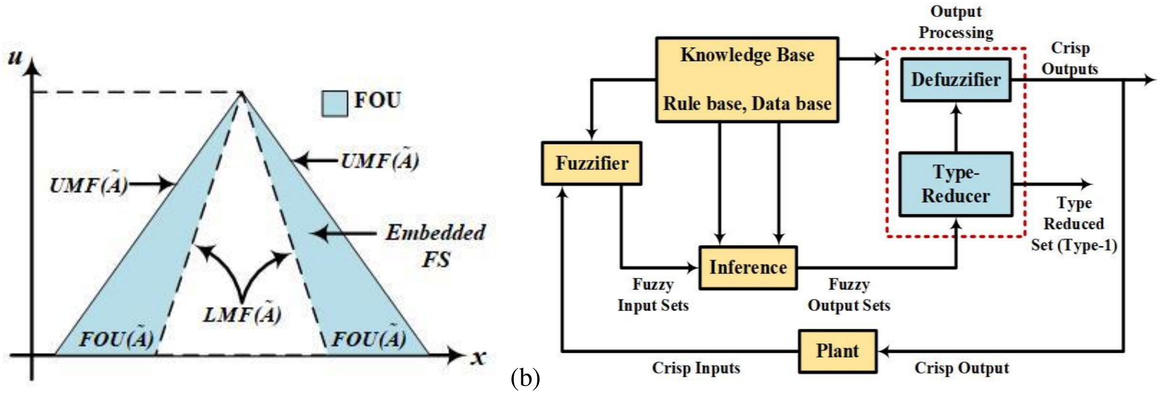

(a) (b)

Fig. 1. (a) Interval Type-2 fuzzy MF (b) Control diagram of an IT2FLS

2. Rule Base

The rule base of IT2FLS are similar to T1FLS and are formulated based on the user's knowledge.

Basically, the r^{th} rules of IT2FLS are expressed as follows:

$$R^j : \text{If } e_1 \text{ is } \tilde{F}_1^r \text{ and } e_2 \text{ is } \tilde{F}_2^r \text{ then } y \text{ is } \tilde{G}^i : \quad r=1,...,P. \tag{16}$$

Where, $\tilde{F}_i^r, \tilde{G}^r$ are the input states, e_1,e_2 are the inputs whereas y is the output. P denotes the rules.

3. Inference

The inference engine in IT2FLS combines the rules to generate the output. Here, a product t-norm based inference engine is adopted and is given by:

$$F^r(x) = \left[\underline{f}^r(x), \overline{f}^r(x)\right] \tag{17}$$

Where, $\underline{f}^r(x) = \underline{\mu}_{\tilde{F}_1^r}(x_1) \times \underline{\mu}_{\tilde{F}_2^r}(x_2)$ and $\overline{f}^r(x) = \overline{\mu}_{\tilde{F}_1^r}(x_1) \times \overline{\mu}_{\tilde{F}_2^r}(x_2)$.

4. Type Reducer

The function of type reducer is to reduce the type of T2FS to T1FS. Here, a centre of sets (COS) type reducer is adopted and is given by:

$$Y_{\cos}(x) = \int_{y^1 \in Y^r} \cdots \int_{y^N \in Y^r} \int_{f^1 \in F^r(x)} \cdots\cdot \int_{f^N \in F^r(x)} \left[\sum_{r=1}^{N} f^r \Big/ \sum_{r=1}^{N} f^r y^r \right] = [y_l, y_r] \tag{18}$$

The expression of two end points (y_l) and (y_r) are computed as follows:

$$y_l = \sum_{r=1}^{N} f_l^r y_l^r \Big/ \sum_{r=1}^{N} f_l^r \tag{19}$$

$$y_r = \sum_{r=1}^{N} f_r^r y_r^r \Big/ \sum_{r=1}^{N} f_r^r \tag{20}$$

5. Defuzzification

In defuzzification process, the crisp inputs are extracted from type reduced T1FS. This process computed by taking average of the end points.

$$y_{output}(x) = \frac{y_l + y_r}{2} \tag{21}$$

3.2. Sliding Mode Control based Power System Stabilizer (SMC-PSS)

SMC is a most promising robust control approach that offer superior disturbance rejection characteristics under parametric variations and uncertainties. The execution of SMC involves two phases such as reaching and sliding phase. Out of these phases, the system is exposed to disturbances in reaching phase of SMC. Hence, exclusion of reaching phase enhances system stability [23]-[27].The purpose of SMC is to keep the error on the sliding surface by neglecting the consequences of reaching phase and chattering.

The nonlinear model of power system under disturbance is expressed as [23]:

$$\begin{cases} \dot{x}_1 = x_2 \\ \dot{x}_2 = f(x,t) + g(x,t)u \end{cases} \tag{22}$$

Where, $x(t) \in R^n$ and $u(t) \in R^m$ are state and control vectors, $f(x)$ is a nonlinear function. Here, state vector, $x = [\Delta\omega \quad \Delta P/M]^T \in R^2$; where $\Delta P = P_m - P_e$, $u \in R$ is the input signal.

The tracking error *(e)* is the difference among trajectory state (x) and command (x_d) is given by:

$$e = x_d - x \tag{23}$$

The sliding surface of SMC is expressed as follows:

$$S = x_2 + \beta x_1 - e^{-1}\left(x_2(0) + \beta x_1(0)\right) \tag{24}$$

Where, β is a constant, $x_1(0), x_2(0)$ are the states.

Taking time derivative of Eq. (24) as

$$\dot{S} = \dot{x}_2 + \beta x_2 + e^{-1}\left(x_2(0) + \beta x_1(0)\right) \tag{25}$$

Using Eq. (25), the condition in Eq. (26) can be satisfied using the following theorems.

$$S\dot{S} < 0 \tag{26}$$

Theorem-1: *For the nonlinear system expressed in Eq. (20), a control law is selected by neglecting the effects of reaching phase.*

$$u = -g^{-1}(x)\left(f(x) + \beta x_2 + e^{-1}\left(x_2(0)\right) + \frac{S}{\rho^2}\right); \quad \rho > 0 \tag{27}$$

Proof: The Lyapunov function (V) is given by:

$$V = \frac{1}{2} S^T S\ , \tag{28}$$

Where, S, S^T denote sliding surface and its transpose.

Substituting Eq. (24)-(25) in Eq. (28) and taking time derivative we get:

$$\begin{aligned} \dot{V} &= S^T \dot{S} \\ &= S\left[\dot{x}_2 + \beta x_2 + e^{-1}\left(x_2(0) + \beta x_1(0)\right)\right] \\ &= S\left[f(x) + g(x)u + \beta x_2 + e^{-1}\left(x_2(0) + \beta x_1(0)\right)\right] \\ &= -\left(\frac{S}{\rho}\right)^2 \end{aligned} \tag{29}$$

For stability, following criterion must be satisfied.

$$\dot{V} \le 0 \tag{30}$$

Remark-1: In the Control law expressed in Eq. (27), calculation of ρ is difficult and tedious process and cannot be computed directly. Again, calculation of $f(x,t)$ and $g(x,t)$ are also difficult. Therefore, a modified control law is presented in the next subsection to overcome the above limitations.

3.3. Adaptive Interval Type-2 Fuzzy Sliding Mode Power System Stabilizer

AIT2FSMC is a modification of AFSMC by type-2 fuzzy systems. The details of AIT2FSMC-PSS can be found in [36]. In this paper, the concept of AIT2FSMC is used for designing a stabilizer for damping out LFEOs under disturbance conditions. The proposed AIT2FSMC-PSS can easily handle nonlinearities and uncertainties of power system and has the unique ability to estimate the nonlinear functions [36].

The nonlinear functions, $f\left(x,t\right)$ and $g\left(x,t\right)$ estimated using universal approximation theorem (UAT) is given by:

$$\hat{f}\left(x,\theta_f\right)=\xi^T\left(x\right)\theta_f \tag{31}$$

$$\hat{g}\left(x,\theta_g\right)=\xi^T\left(x\right)\theta_g \tag{32}$$

Where, $\theta=\left[\theta_1,\theta_2,......\theta_m\right]$, $\xi=\left[\xi_1,\xi_2,......\xi_m\right]$represent vectors of parameter and fuzzy basis function (FBF).

$$\xi^T\theta_f=\frac{1}{2}\left[\xi_r^T\,\xi_l^T\right]\left[\theta_{fr}\theta_{fl}\right] \tag{33}$$

$$\xi^T\theta_g=\frac{1}{2}\left[\xi_r^T\,\xi_l^T\right]\left[\theta_{gr}\theta_{gl}\right] \tag{34}$$

Where, $\xi_l=\left[\xi_l^1,\xi_l^2,.....,\xi_l^m\right]^T$, $\xi_r=\left[\xi_r^1,\xi_r^2,.....,\xi_r^m\right]^T$, $\theta_r=\left[\theta_{1r},\theta_{2r},.....,\theta_{mr}\right]$and $\theta_l=\left[\theta_{1l},\theta_{2l},.....,\theta_{ml}\right]$.

The approximation error $\left(\varepsilon\right)$ as:

$$\varepsilon=\delta_f+\delta_g u \tag{35}$$

Where,

$$\delta_f=f\left(x\right)-\xi^T\left(x\right)\theta_f^* \tag{36}$$

$$\delta_g=g\left(x\right)-\xi^T\left(x\right)\theta_g^* \tag{37}$$

Where, θ_f^*, θ_g^* are optimal approximation parameters.

$$\tilde{\theta}_f=\theta_f-\theta_f^* \tag{38}$$

$$\tilde{\theta}_g=\theta_g-\theta_g^* \tag{39}$$

Theorem-2: *To ensure stability and robustness, a modified control law is selected.*

$$u=-\hat{g}^{-1}\left(x\right)\left(\hat{f}\left(x\right)+\beta x_2+e^{-1}\left(x_2\left(0\right)+\beta x_1\left(0\right)\right)+\frac{S}{\rho^2}\right) \tag{40}$$

The adaptation laws are given below:

$$\dot{\theta}_f=\gamma_1 S\xi\left(x\right)-\gamma_1\theta_f \tag{41}$$

$$\dot{\theta}_g=\gamma_2 S\xi\left(x\right)-\gamma_2\theta_g \tag{42}$$

Proof:

Selecting the Lyapunov function (*V*) as:

$$V=\frac{1}{2}S^T S+\frac{1}{2\gamma_1}\tilde{\theta}_f^T\tilde{\theta}_f+\frac{1}{2\gamma_2}\tilde{\theta}_g^T\tilde{\theta}_g \tag{43}$$

Applying time derivative to Eq. (43), we get:

$$\begin{aligned}\dot{V}&=S^T\dot{S}+\frac{1}{2\gamma_1}\tilde{\theta}_f^T\dot{\theta}_f+\frac{1}{2\gamma_2}\tilde{\theta}_g^T\dot{\theta}_g\\&=S^T\left(\dot{x}_2-\hat{g}\left(x,\theta_g\right)u-\hat{f}\left(x,\theta_f\right)-\frac{S}{\rho^2}\right)+\frac{1}{\gamma_1}\tilde{\theta}_f^T\dot{\theta}_f+\frac{1}{\gamma_2}\tilde{\theta}_g^T\dot{\theta}_g\end{aligned} \tag{44}$$

$$= S^T\left(-\left(\hat{f}\left(x,\theta_f\right)-f\left(x\right)\right)-\left(\hat{g}\left(x,\theta_g\right)-g\left(x\right)\right)u-\frac{S}{\rho^2}\right)+\frac{1}{\gamma_1}\tilde{\theta}_f^T\dot{\theta}_f+\frac{1}{\gamma_2}\tilde{\theta}_g^T\dot{\theta}_g$$

$$= S^T\left(-\tilde{\theta}_f^T\xi\left(x\right)-\tilde{\theta}_g^T\xi\left(x\right)u+\varepsilon-\frac{S}{\rho^2}\right)+\frac{1}{\gamma_1}\tilde{\theta}_f^T\dot{\theta}_f+\frac{1}{\gamma_2}\tilde{\theta}_g^T\dot{\theta}_g$$

Substituting the adaptation laws mentioned in Eq. (41)-Eq. (44), we get:

$$\dot{V} = -\frac{S}{\rho^2}-\tilde{\theta}_f^T\dot{\theta}_f-\tilde{\theta}_g^T\dot{\theta}_g+\varepsilon S \tag{45}$$

The inequality conditions are given below:

$$-\tilde{\theta}_f^T\theta_f \le \frac{1}{2}\tilde{\theta}_f^T\theta_f+\frac{1}{2}\left\|\theta_f^*\right\|^2 \tag{46}$$

$$-\tilde{\theta}_g^T\theta_g \le \frac{1}{2}\tilde{\theta}_g^T\theta_g+\frac{1}{2}\left\|\theta_g^*\right\|^2 \tag{47}$$

Now, the expression of $\dot{V}$ is given by:

$$\dot{V} \le \left(\frac{S}{\rho^2}+\frac{1}{2}\tilde{\theta}_f^T\tilde{\theta}_f+\frac{1}{2}\tilde{\theta}_g^T\tilde{\theta}_g\right)+\left\|\varepsilon S\right\|+\frac{1}{2}\left\|\theta_f^*\right\|^2+\frac{1}{2}\left\|\theta_g^*\right\|^2 \tag{48}$$

Assuming, $\alpha = \min\left(\frac{2}{\rho^2},\gamma_1,\gamma_2\right)$ and $\mu = \frac{1}{2}\left\|\theta_f^*\right\|^2+\frac{1}{2}\left\|\theta_g^*\right\|^2+\left\|\varepsilon S\right\|$.

$$\dot{V} \le -\alpha V+\mu \tag{49}$$

Multiplying both sides of Eq. (49) by e^{at}, we get:

$$\frac{d}{dt}\left(Ve^{at}\right) \le \mu e^{at} \tag{50}$$

Integrating Eq. (50) in the range between 0 to t:

$$0 \le V\left(t\right) \le \left(V\left(0\right)-\frac{\mu}{\alpha}\right)e^{at}+\frac{\mu}{\alpha} \tag{51}$$

$$0 \le V\left(t\right) \le V\left(0\right)+\frac{\mu}{\alpha} \tag{52}$$

$$0 \le V\left(t\right) \le \eta \tag{53}$$

$$\eta = V\left(0\right)+\frac{\mu}{\alpha} \tag{54}$$

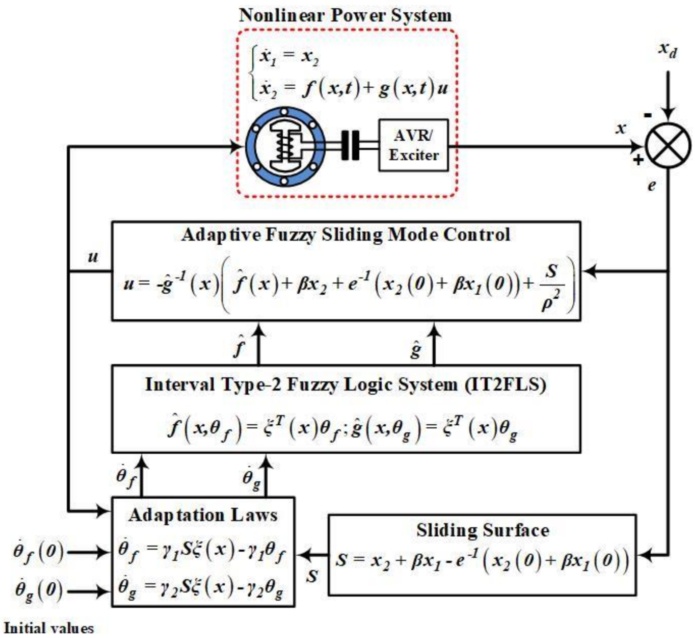

Fig. 2. Control process of the proposed AIT2FSMC-PSS.

Applying Barbalat's Lemma, it is found that, sliding surface (S) and derivative of sliding surface $(\dot{S})$ are bounded and also small approximation error (ε), $\tilde{\theta}_f$ and $\tilde{\theta}_g$ are also bounded. The control process of the proposed AIT2FSMC-PSS is depicted in Fig. 2.

The proof is completed.

Remark-2: It is clear that, the proposed control scheme satisfies the stability criterion and the error asymptotically converges to zero.

4. Simulation Results and Discussion

In this section, the viability of the proposed AIT2FSMC-PSS is analysed under uncertainties and disturbances. The proposed scheme is implemented using MATLAB/ Simulink environment and verified in both single and multimachine power systems. Different small and transient disturbance scenarios are considered to analyse the performance of the proposed AIT2FSMC-PSS and the results are compared with AFSMC-PSS, SMC-PSS, FPSS and CPSS based on their PIs, Eigen values, damping ratios, oscillating frequencies, ITAE and FD. The inputs to the proposed stabilizer are speed deviation $(\Delta\omega)$ and accelerating power (ΔP). Type-2 fuzzy triangular MFs shown in Fig. 3 (a)-(b) are considered for the stability analysis. 25 fuzzy rules with 05 linguistic variables like negative big (NEB), negative medium (NEM), zero (ZER), positive medium (POM) and positive big (POB) given in Table-1 are considered.

Table-1 Type-2 fuzzy rule base

		ΔP				
		NEB	NEM	ZER	POM	POB
$\Delta\omega$	NEB	POB	POB	ZER	ZER	POM
	NEM	POM	POB	NEB	POM	NEB
	ZER	POB	POM	NEB	NEB	ZER
	POM	ZER	POB	ZER	NEB	ZER
	POB	ZER	ZER	POB	POM	POM

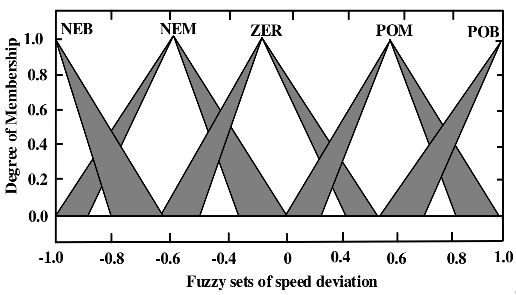

(a)

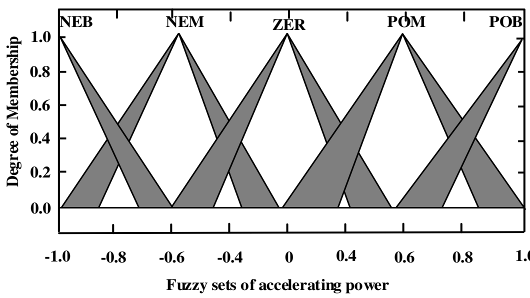

(b)

Fig. 3 Membership functions of IT2FLC (a) speed deviation (b) accelerating power

Small signal stability analysis is executed on a linearized model of power system. The state equations are framed from the state space model of the linearized system and the corresponding Eigen values, damping ratios and oscillating frequencies are obtained. From the location of Eigen values in the S-plane, the stabilities of the power system can be analysed.

The procedure for calculating Eigen values, damping ratios and oscillating frequencies are as follows:

From the characteristics equation given in Eq. (55), the Eigen values (λ) can be calculated as follows:

$$\det(sI - A) = 0 \tag{55}$$

$$\det(A - \lambda I) = 0 \tag{56}$$

$$\lambda = eig(A) \tag{57}$$

The expression for calculating damping ratio (ξ) and oscillation frequency (σ) is given by [23]:

$$\delta_i = real(\lambda_i), \quad i = 1.2, ..., n \tag{58}$$

$$\xi_i = -\delta_i \Big/ \sqrt{\delta_i^2 + \beta_i^2}, \quad i = 1.2, ..., n \tag{59}$$

$$\sigma_i = \frac{\beta_i}{2\pi}, \quad i = 1.2, ..., n \tag{60}$$

The expression for calculating ITAE and FD are given as follows [40]:

$$ITAE = \sum_{i=1}^{N_{SD}} \int_0^{t_{sim}} t.\left(\left|(\Delta\omega)_i\right|\right) dt \tag{61}$$

$$FD = \frac{1}{N_{SD}} \sum_{i=1}^{N_{FD}} \left((3000 \times MP_i)^2 + (3000 \times US_i)^2 + (T_{s,i})^2 \right) \tag{62}$$

Where, N_{FD} is the number of signals, MP, US, denote the under and overshoots, T_s is the settling time.

4.1. Single Machine Infinite Bus (SMIB) Power System

This sub-section, the assessment of stability is performed in SMIB system as given in Fig. 4. The SMIB system comprises of a 200 MVA synchronous generator feeding power to the infinite bus (rest power system) through 100 km line. As, the power system is an elementary one, it can give an idea of small signal stability under various uncertainties and disturbance conditions.

To testify the efficacy and robustness of the proposed stabilizer and to determine its supremacy over aforesaid stabilizers, 04 different disturbance scenarios are considered. The disturbances are selected that, they cover the uncertainties and disturbances of the power system. The disturbance scenarios in SMIB power system are as follows:

- *Scenario-1*: Normal loading with 5% increase in line parameters.
- *Scenario*-2: 10% increase in loading and 10% increase in line parameters.
- *Scenario*-3: 20% increase in loading and 15% increase in line parameters.
- *Scenario*-4: A 3-ϕ fault in the transmission line.

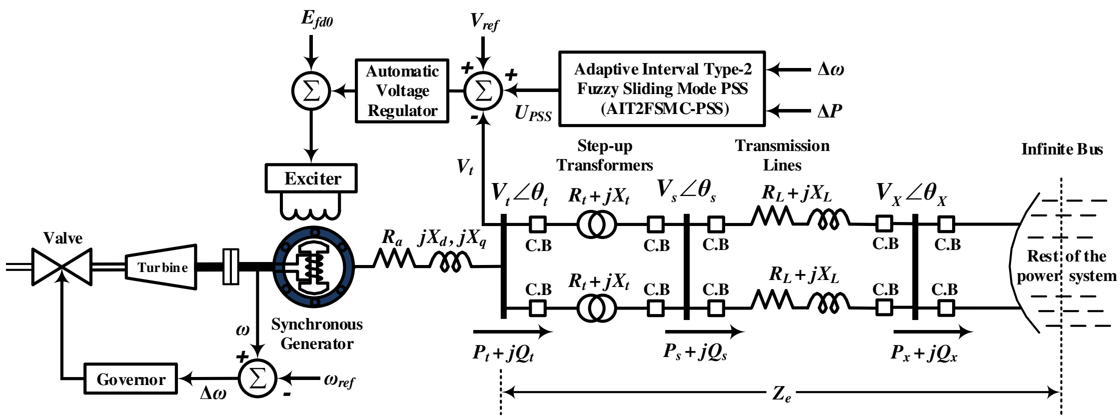

Fig. 4. Structure of SMIB power system.

With the increase in loading conditions, stability margin gets reduced and entire system is pushed towards instability. In this regard, a gradual increase in loading by 5%, 10% and 15% is applied at t=0 seconds for the first three disturbance scenarios. The impacts of variations in loading and transmission line parameters are observed in deviations in speeds of corresponding synchronous generators. In scenario-1, under normal loading condition and 5% increase in line parameters, the speed deviations depicted in Fig. 5 (a) are maximum in case of CPSS and the oscillations go on reducing with the presented stabilizers. The proposed AIT2FSMC-PSS show minimum peak and settling characteristics with maximum of Eigen values, damping ratios and ensure superior oscillating damping performance. Similarly, in scenario-2 and scenario-3, the loadings are increased by 10% and 20% and the transmission line parameters are increased by 10% and 15%. As observed from the simulated responses depicted in Fig. 5 (b) and Fig. 5 (c), that the increase in loading and line parameters greatly impacts the stability of the power system. The system is highly oscillatory under these disturbance scenarios. Maximum oscillations are present in case of CPSS and also settling time is quite high than other stabilizers. The Eigen values and its corresponding damping ratios are very close to the origin of s-plane. The performance of CPSS under these disturbances are close to instability. Again, there are oscillations observed in case FPSS, FSMC-PSS and AFSMC-PSS. But, the proposed AIT2FSMC-PSS easily manages the disturbances with minimum peak values and settling time than other stabilizers. Again, Eigen values and electromechanical modes damping ratios are found to be shifted well within the left half of s-plane which assures stability of the proposed stabilizer. In scenario-4, the most severe fault called 3ϕ fault is applied as a disturbance. The simulated response is given in Fig. 5 (d). While accessing stability of the proposed stabilizer under this severe fault disturbance, it is observed that the system is oscillatory. Especially, CPSS possesses maximum settling time and overshoot time than others. Again, while comparing the Eigen values, it is clear that the roots are closer to unstable region than other stabilizers. Whereas, the proposed stabilizer shows superior oscillation damping characteristics with minimum of settling time of 2.34 seconds and peak overshoot of 4.6 p.u. to that of other stabilizers. The comparison of Eigen values, damping ratios and oscillating frequencies of SMIB system under the aforementioned disturbance scenarios are presented in Table-2.

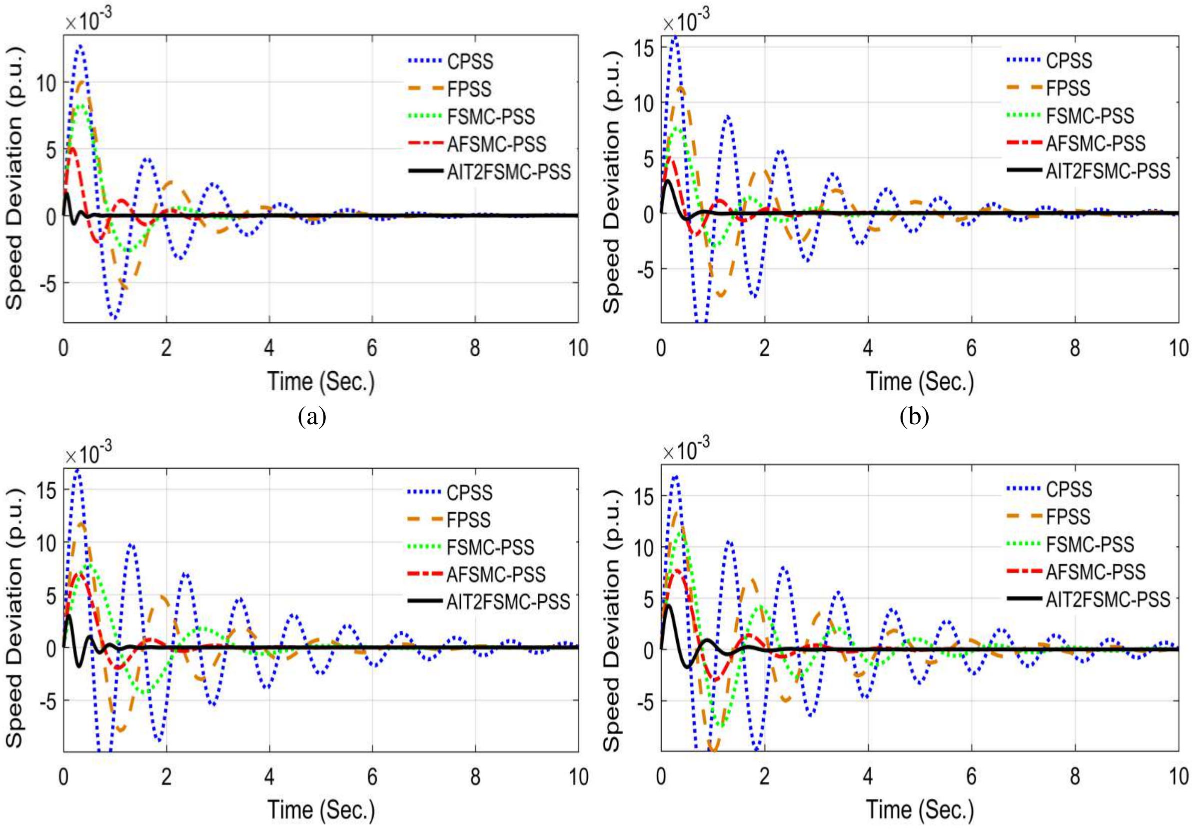

(a) (b) (c) (d)

Fig. 5. Simulation response of SMIB system under (a) scenario-1 (b) scenario-2 (c) scenario-3 (d) scenario-4

Table 2 Comparison of Eigen value for SMIB system

Disturbances	Methodology	Eigen values	Damping ratios
Scenario-1	**IT2AFSMC-PSS**	**-3.864 ± j9.365**	**0.758**
	AFSMC-PSS	-3.152 ± j6.325	0.568
	FSMC-PSS	-1.221 ± j4.256	0.335
	FPSS	-0.684 ± j3.256	0.221
	CPSS	-0.225 ± j2.256	0.063
Scenario-2	**IT2AFSMC-PSS**	**-3.635 ± j7.985**	**0.535**
	AFSMC-PSS	-2.365 ± j5.745	0.498
	FSMC-PSS	-1.745 ±j4.201	0.274
	FPSS	-0.965 ±j3.246	0.154
	CPSS	-0.365 ±2.632	0.067
Scenario-3	**IT2AFSMC-PSS**	**-3.689± j7.855**	**0.458**
	AFSMC-PSS	-2.722± j6.325	0.357
	FSMC-PSS	-1.985± j5.214	0.254
	FPSS	-1.652 ±j4.226	0.091
	CPSS	-0.632 ±j1.568	0.021
Scenario-4	**IT2AFSMC-PSS**	**-3.932 ± j6.819**	**0.653**
	AFSMC-PSS	-3.013 ± j5.442	0.452
	FSMC-PSS	-2.766 ± j4.128	0.376
	FPSS	-2.119 ±j3.917	0.153
	CPSS	-1.766 ±j1.766	0.118

4.2. Multimachine Power System

In this sub-section, the viability of the proposed stabilizer is implemented in a 16-machine, 68-bus power system to illustrate its efficacy in a multimachine power system. Fig. 6 shows the studied multimachine power system comprising 16-generators, 25 transformers and 83 transmission lines and are divided into five areas located at different geographical regions as shown in Fig. 2. The five areas of MMPS are New England Power System (NEPS) in area-5 comprising of generators (G1-G8), New York Power System (NYPS) in area-3 comprising of generators (G9-G12) and three areas consisting of generators G13, G14 and G15. The five areas are linked with each other through tie-lines for assuring smooth interarea power flow. The generators in different areas will swing against each other and undergo local and interarea mode oscillations followed by a disturbance.

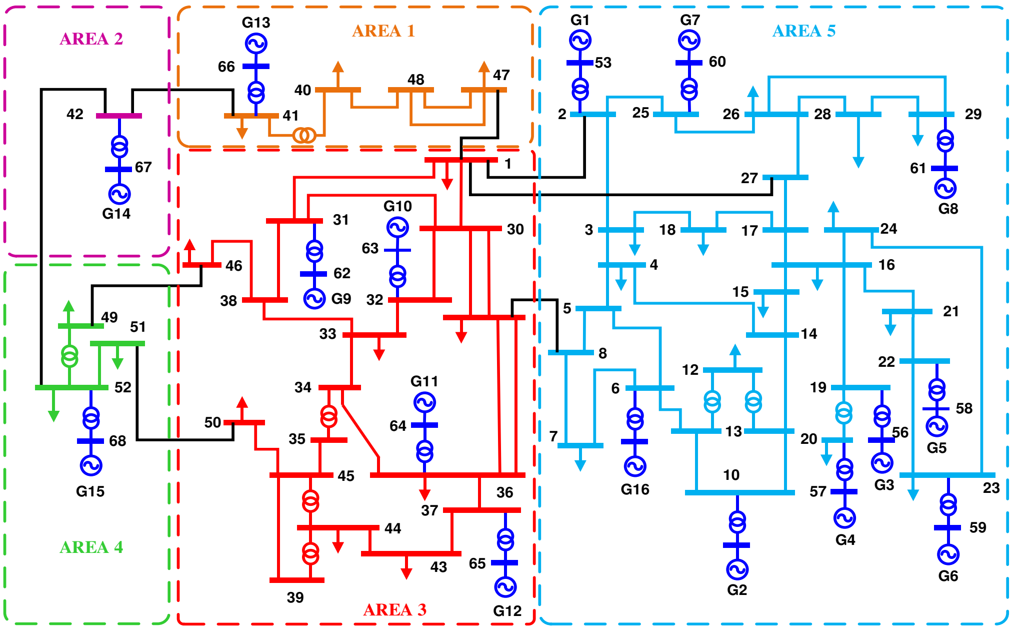

Fig. 6. Structure of multimachine power system [38].

Different disturbance scenarios are considered to testify the effectiveness of the proposed stabilizer are mentioned in the subsequent subsections. The simulation results in terms of speed deviations for different disturbances are shown in Fig. (7)-(10) respectively. A performance comparison is performed for the proposed AIT2FSMC-PSS (black colour bold line), AFSMC-PSS (red colour dash-dot line), FSMC-PSS (green colour dotted line), FPSS (brown colour dashed line) and CPSS (blue colour dotted line).

4.2.1. Small Signal Stability Analysis

In this sub-section, analysis of small signal stability of the proposed AIT2FSMC-PSS is performed for small disturbance. A 10% step increase in load demand is applied to bus-21 of area-5 at t=1 second and the corresponding speed deviation in generators G_{13}, G_{14}, G_{15}, G_{12} and G_5 located at deferent areas of MMPS representing local mode of oscillations are given in Fig. 7 (a)-(e) respectively. The simulation responses of different generators reveal that the proposed AIT2FSMC-PSS is efficient in damping LFEOs than that of AFSMC-PSS, FSMC-PSS, FPSS and CPSS. This establishes the effectiveness of the proposed AIT2FSMC-PSS in the improvement small signal stability with lesser oscillations in peak overshoot and settling time.

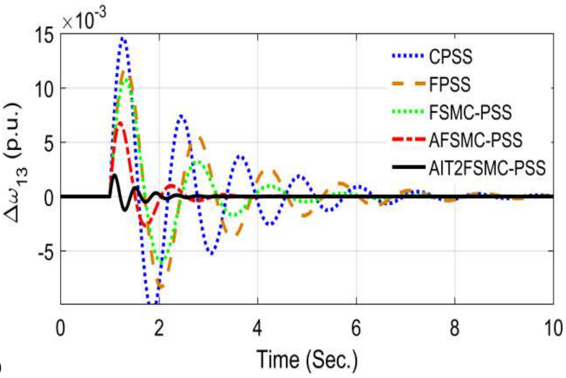

(a)

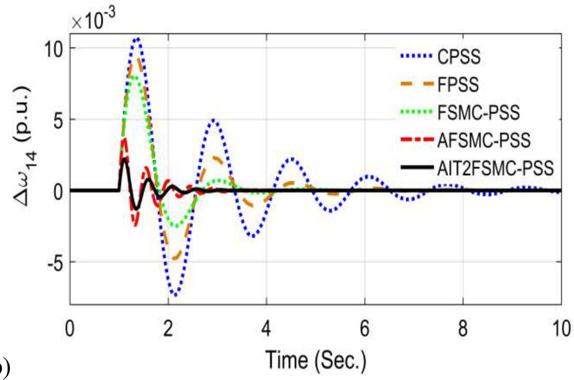

(b)

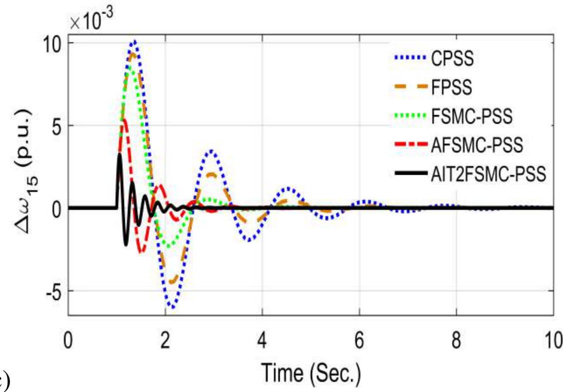

(c)

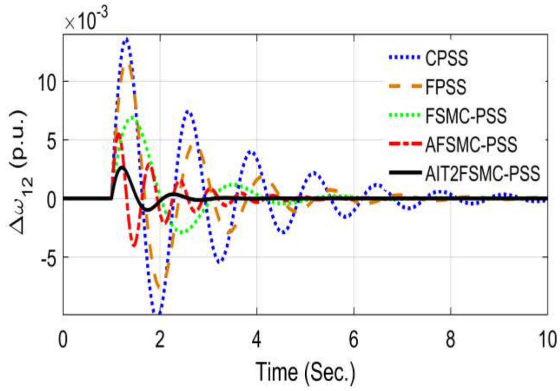

(d)

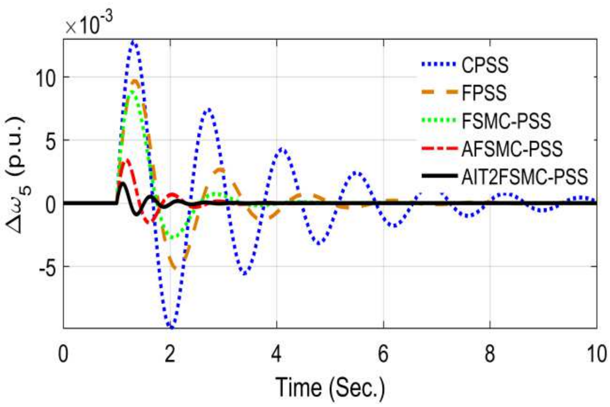

(e)

Fig. 7. Speed deviation in (a) G_{13} of area-1 (b) G_{14} of area-2 (c) G_{15} of area-3 (d) G_{12} of area-4 (e) G_5 of area-5.

4.2.2. Transient Stability Analysis

In this sub-section, investigation of transient stability is performed to validate the efficacy of the proposed stabilizer in handling transient disturbances like 3-ϕ faults. Different disturbances considered for the analysis of transient stability are as follows:

- *Scenario-1*: 3-ϕ fault of 100ms duration is applied at bus-36 of area-3.
- *Scenario-2*: A 6-cycle 3-ϕ fault at bus-18 of area-5.
- *Scenario-3*: A line outage between bus-30-31 of area-5.

The simulations are performed for various speeds deviations of generators located at different geographical areas showing local and interarea oscillations are presented in Fig. (8)-(10) respectively. The stability analysis under these aforementioned fault disturbances are discussed below.

In scenario-1, a 3-ϕ fault disturbance of 200ms duration is created at bus-36 of area-3 at t=1 seconds to analyse the stability performance. Under this severe fault disturbance, the system undergoes oscillations which is replicated through deviations in speeds of synchronous generators at different areas. To analyse the stabilities of the proposed AIT2FSMC-PSS, difference in speed deviations between generators of different areas such as G_{10}-G_{13}, G_9-G_{12} and G_{15}-G_3 representing local and interarea mode oscillations are shown in Fig. 8 (a)-(c) are considered. The simulated responses clearly shows the impact of 3-ϕ fault disturbance with maximum oscillations in the speed of the generators. The speed deviation using CPSS is highly oscillatory in all the three cases and the oscillations go on reducing in case of FPSS, FSMC-PSS and AFSMC-PSS. But, the proposed AITFSMC-PSS easily tackle the severe fault disturbance and show minimum oscillations in peak overshoot and settling time. The Eigen value analysis under this disturbance scenario is presented in Table-3. By verifying the Eigen values and damping ratios, it clearly seen that, the Eigen are values well within the left of the S-plane in case of the proposed AITFSMC-PSS. This conforms the stability of the proposed stabilizer.

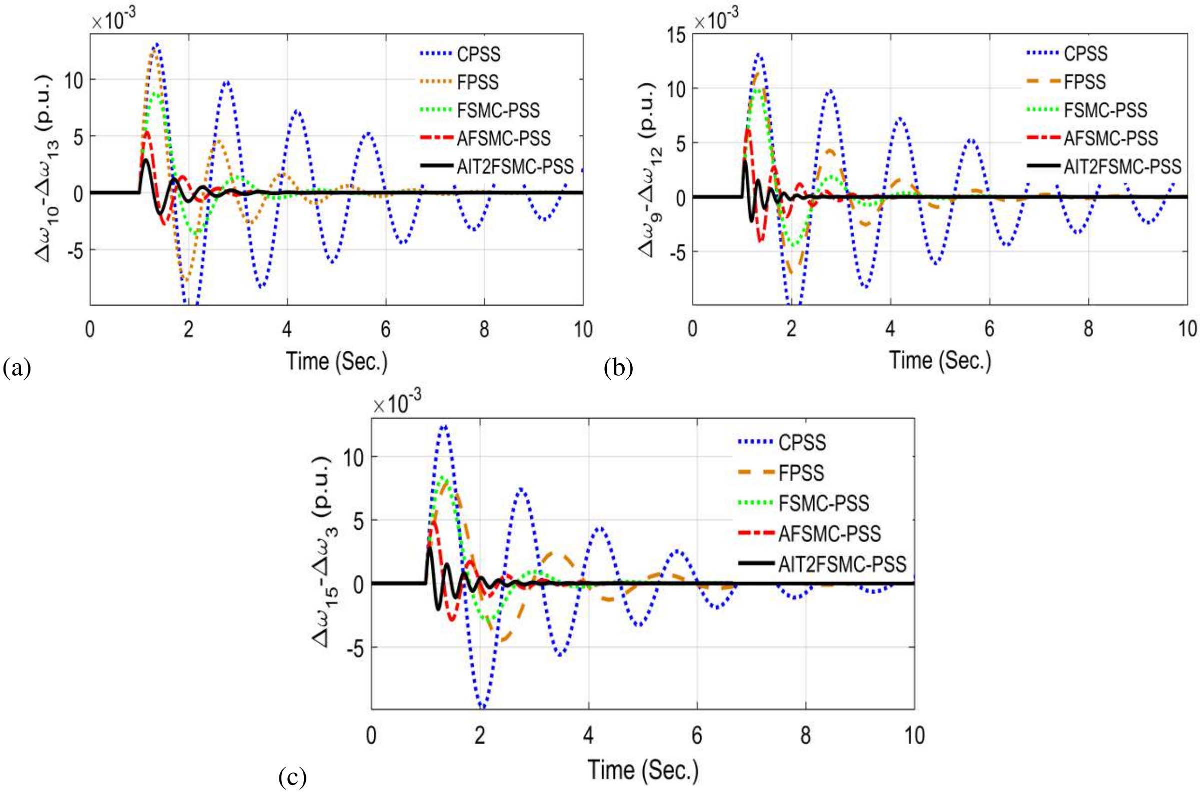

Fig. 8. Speed deviation in scenario-1

In scenario-2, a 6-cycle, 3-ϕ fault disturbance is created at bus-18 of area-5 at t=1 seconds. The resulting speed deviations among G_{10}-G_{13}, G_3-G_7 and G_1-G_{14} representing local and interarea mode oscillations under the aforementioned fault disturbance are depicted in Fig. 9 (a)-(c) respectively. Under this fault disturbance, the speeds of the synchronous generators oscillates from its rated speed. But, due to the application of proposed stabilizers, these oscillations settle back to their nominal value of 1 p.u. More oscillations are seen in case of CPSS whereas comparatively lesser in case of FPSS, FSMC-PSS, and AFSMC-PSS. The proposed AITFSMC-PSS shows minimum oscillations with minimum peak values and settling time to that of other approaches. Again, Eigen value analysis presented in Table-4 also supports the stability study. It is seen that the roots are more negative in case of AIT2FSMC-PSS than that of other stabilizers. This proves the efficacy and effectiveness of the proposed stabilizer handling transient disturbances and enhancing stability under a 3-ϕ fault disturbance.

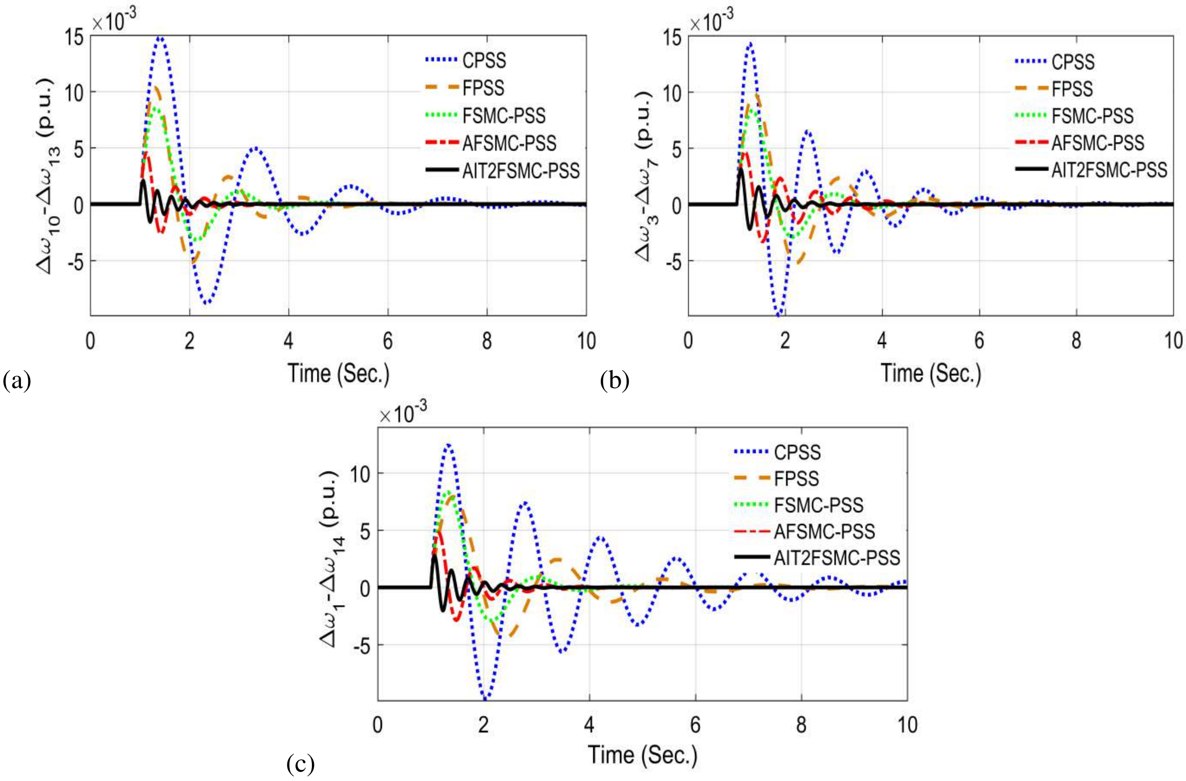

Fig. 9. Speed deviation in scenario-2

In scenario-3, the effectiveness of the proposed AIT2FSMC-PSS is studied for a line outage disturbance. In this scenario, the line connecting bus-30-31 of area-5 is tripped at t=1 seconds and reclosed after 3-cycles. The corresponding speed deviations between generators G_{11}-G_{13}, G_{10}-G_{12} and G_{15}-G_3 representing local and interarea mode oscillations under the aforementioned fault disturbance are depicted in Fig. 10 (a)-(c) respectively. The impact of line outage disturbance is reflected on the simulation results, as it undergoes oscillations in speed deviations. The proposed approaches efficiently damps out the oscillations under this fault disturbance. The response of CPSS is quite oscillatory to that of FPSS, FSMC-PSS and AFSMC-PSS. The proposed AIT2FSMC-PSS exhibits efficient oscillation damping with minimum of peak values and settling characteristics. Again, Eigen value analysis in Table-5 supports the stability as that the roots are shifted towards left half of S-pale in case of proposed AIT2DSMC-PSS. This proves the robustness of the proposed approach in handling the line outage disturbance.

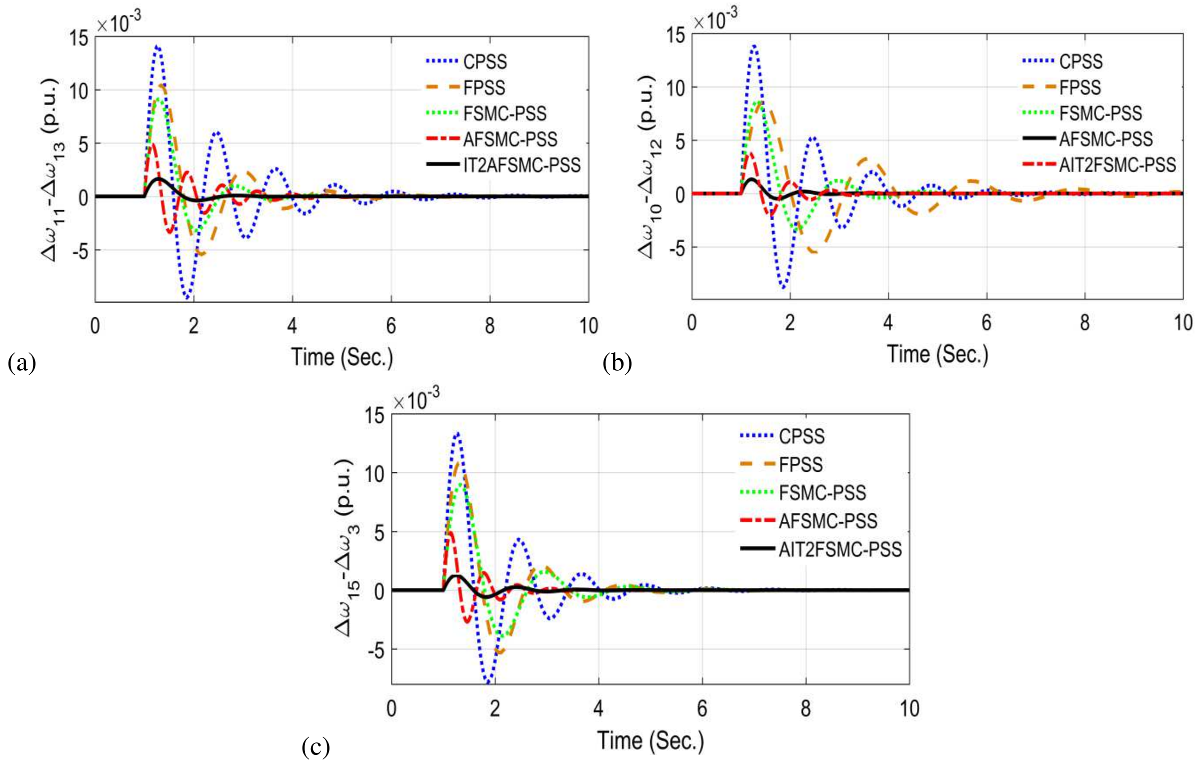

Fig. 10. Speed deviation in scenario-3

Table-3 Comparison of Eigen value for scenario-1

Modes	λ	ξ	σ
Local mode	**-3.256 ±j5.325**	**5.356**	**2.359**
	-2.658± j3.895	7.689	1.958
	-1.635 ±j6.328	5.254	1.476
	-1.012 ±j7.256	6.457	0.957
	-0.785 ±1.257	11.35	0.663
Interarea mode	**-1.856 ±j5.458**	**2.358**	**0.985**
	-1.325± j2.359	18.22	0.689
	-0.635 ±j4.258	23.25	0.224

Table-4 Comparison of Eigen value for scenario-2

Modes	λ	ξ	σ
Local mode	**-3.256 ±j6.375**	**6.778**	**2.214**
	-2.985± j4.235	6.325	2.023
	-2.487 ±j8.658	7.259	1.758
	-2.024 ±j6.325	4.265	1.359
	-1.568 ±j8.112	7.968	0.958
Interarea mode	**-1.985 ±j6.358**	**3.258**	**0.884**
	-1.487± j6.359	20.38	0.698
	-0.368 ±j8.859	17.89	0.227

Table-5 Comparison of Eigen value for scenario-3

Modes	λ	ξ	σ
Local mode	**-3.256 ± 2.658**	**5.365**	**2.689**
	-2.968± j4.226	6.598	2.359
	-2.389 ±j7.635	4.238	1.987
	-1.895 ±j7.859	6.658	1.256
	-0.759 ±j6.325	10.86	0.658
Interarea mode	**-1.764 ±j3.256**	**2.598**	**0.968**
	-0.927± j2.598	23.27	0.538
	-0.685 ±j7.256	19.84	0.157

4.3. Uncertainty Analysis

This section is presented to confirm the viability of the proposed AIT2FSMC-PSS in handling uncertainties of power system. Uncertainties are due to error in measurement, disturbances, parameter variations, noise etc. The AI2TFSMC-PSS has shown its effectiveness in tackling various small and transient disturbances. In order to verify the performance of AIT2FSMC-PSS to deal with uncertainties, a random noise is supplemented with the input signal $e(t)$ [23].

$$e(t) = e(t) + \gamma \times \text{randn} \tag{50}$$

Where, randn denotes random numbers, γ represents uncertainty level and its value is taken as 0.05 [34].

The simulation results are presented in Fig. 11 (a)-(c) respectively. As observed, the proposed stabilizer can easily handles the noise present in the power system and it shows lesser peak and settling characteristics to the response of the stabilizer with noise. A comparison of ITAE values with and without noise is given in Table-6. Both simulation and comparison proves the effectiveness of AIT2FSMC-PSS in handling uncertainties present in the power system.

Table-6 Comparison of ITAE values

	Scenario-1	Scenario-2	Scenario-3
Without noise	0.38	0.47	0.45
With noise	3.76	5.44	4.37

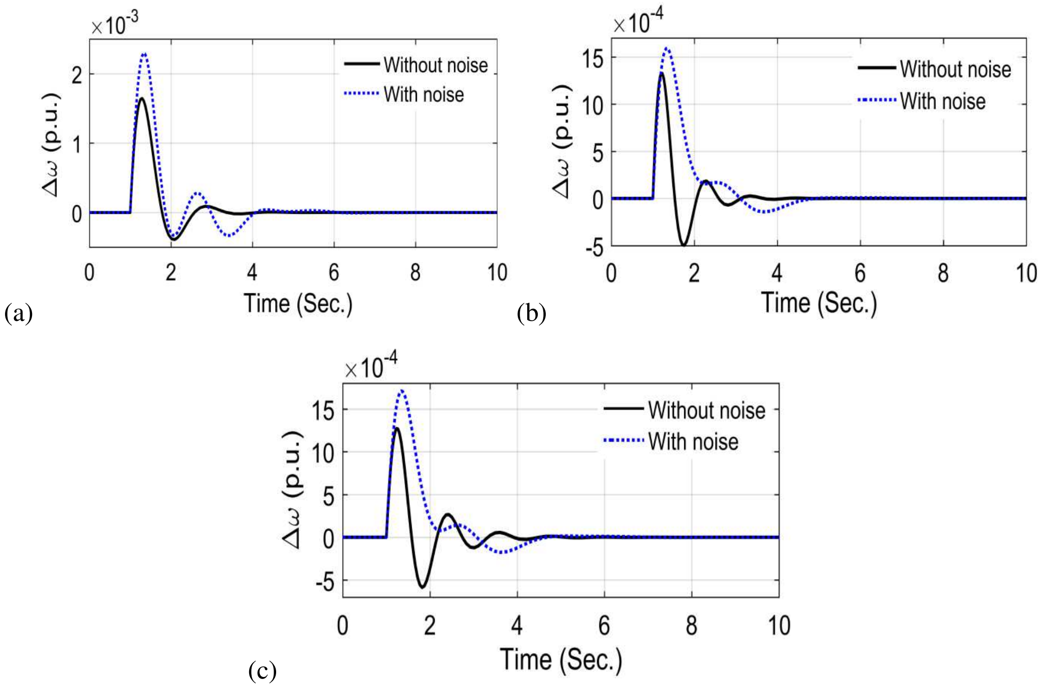

Fig. 11. Simulation response under uncertainties.

4.4. Comparative Analysis

This sub-section presents a quantitative performance analysis of the designed stabilizers. Different PIs like maximum peak overshoot (M_p), settling time (T_s), integral of time absolute error (ITAE) and figure of demerit (FD) are considered for evaluating the performance of the stabilizers. A comparison of PIs of responses of SMIB system under different disturbance scenarios are presented in Table-7. As analysed in the previous subsections, the proposed AIT2FSMC-PSS shows superior oscillation damping with minimum of its PIs under different disturbance scenarios. The results are bolded to show its superiority over others.

Table 7 Comparison of PIs of SMIB power system

Scenarios	Approaches	M_p	T_s
Scenario-1	**AIT2FSMC-PSS**	**1.574×10^{-3}**	**0.731 sec.**
	AFSMC-PSS	4.891×10^{-3}	2.421 sec.
	FSMC-PSS	8.179×10^{-3}	3.555 sec.
	FPSS	9.862×10^{-3}	5.445 sec.
	CPSS	12.64×10^{-3}	7.921 sec.
Scenario-2	**AIT2FSMC-PSS**	**2.862×10^{-3}**	**1.211 sec.**
	AFSMC-PSS	4.961×10^{-3}	2.564 sec.
	FSMC-PSS	7.612×10^{-3}	3.831 sec.
	FPSS	11.21×10^{-3}	7.211 sec.
	CPSS	13.82×10^{-3}	9.862 sec.
Scenario-3	**AIT2FSMC-PSS**	**3.461×10^{-3}**	**1.764 sec.**
	AFSMC-PSS	6.892×10^{-3}	3.142 sec.
	FSMC-PSS	7.874×10^{-3}	4.545 sec.
	FPSS	11.72×10^{-3}	7.412 sec.
	CPSS	16.76×10^{-3}	10.63 sec.
Scenario-4	**AIT2FSMC-PSS**	**4.661×10^{-3}**	**2.344 sec.**
	AFSMC-PSS	8.172×10^{-3}	3.441 sec.
	FSMC-PSS	10.83×10^{-3}	5.912 sec.
	FPSS	13.22×10^{-3}	7.736 sec.
	CPSS	17.46×10^{-3}	13.64 sec.

Table- 8 **S**ignal stability analysis in MMPS

Stability analysis under 10% decrease in load demand										
Approaches	$\Delta\omega_{13}$		$\Delta\omega_{14}$		$\Delta\omega_{15}$		$\Delta\omega_{12}$		$\Delta\omega_{5}$	
	M_p ($\times10^{-3}$)	T_s (sec.)	M_p ($\times10^{-3}$)	T_s (sec.)	M_p ($\times10^{-3}$)	T_s (sec.)	M_p ($\times10^{-3}$)	T_s (sec.)	M_p ($\times10^{-3}$)	T_s (sec.)
AIT2FSMC-PSS	**1.921**	**2.322**	**2.133**	**2.467**	**3.249**	**2.318**	**2.512**	**2.635**	**1.522**	**2.235**
AFSMC-PSS	6.742	3.163	3.699	3.092	5.228	3.114	5.471	4.342	3.363	3.061
FSMC-PSS	10.64	5.098	8.036	4.476	8.384	4.226	7.141	5.871	8.524	3.924
FPSS	11.83	7.589	9.451	6.354	9.239	5.823	11.72	7.402	9.661	6.028
CPSS	14.54	9.814	10.71	9.808	10.06	7.553	13.59	9.509	12.72	10.31

Table- 9 Transient stability analysis in MMPS

Scenario-1: 3-ϕ fault of 100ms applied at bus-36 of area-3.						
Approaches	$\Delta\omega_{10}$ - $\Delta\omega_{13}$		$\Delta\omega_{9}$ – $\Delta\omega_{12}$		$\Delta\omega_{15}$ - $\Delta\omega_{3}$	
	M_p	T_s	M_p	T_s	M_p	T_s
AIT2FSMC-PSS	**2.701×10^{-3}**	**2.733 sec.**	**3.081×10^{-3}**	**2.292 sec.**	**2.715×10^{-3}**	**2.689 sec.**
AFSMC-PSS	5.288×10^{-3}	3.687 sec.	6.611×10^{-3}	3.217 sec.	4.647×10^{-3}	3.506 sec.
FSMC-PSS	8.575×10^{-3}	5.408 sec.	9.676×10^{-3}	4.785 sec.	8.312×10^{-3}	4.844 sec.
FPSS	12.11×10^{-3}	7.204 sec.	11.15×10^{-3}	7.553 sec.	8.019×10^{-3}	7.206 sec.
CPSS	13.04×10^{-3}	14.75 sec.	13.03×10^{-3}	14.44 sec.	12.32×10^{-3}	10.84 sec.
Scenario-2: A 6-cycle, 3-ϕ fault at bus-18 of area-5.						
Methodology	$\Delta\omega_{10}$ - $\Delta\omega_{13}$		$\Delta\omega_{3}$ - $\Delta\omega_{7}$		$\Delta\omega_{1}$ - $\Delta\omega_{14}$	
	M_p	T_s	M_p	T_s	M_p	T_s
AIT2FSMC-PSS	**2.093×10^{-3}**	**2.207 sec.**	**3.099×10^{-3}**	**2.434 sec.**	**2.081×10^{-3}**	**1.713 sec.**
AFSMC-PSS	5.063×10^{-3}	2.828 sec.	4.849×10^{-3}	3.832 sec.	4.288×10^{-3}	2.814 sec.
FSMC-PSS	8.457×10^{-3}	3.973 sec.	8.109×10^{-3}	4.596 sec.	6.346×10^{-3}	4.642 sec.
FPSS	10.33×10^{-3}	5.429 sec.	9.871×10^{-3}	6.858 sec.	9.172×10^{-3}	5.673 sec.
CPSS	14.83×10^{-3}	8.941 sec.	14.22×10^{-3}	8.252 sec.	14.63×10^{-3}	8.211 sec.
Scenario-3: A line outage between bus-30-31 of area-5.						
Methodology	$\Delta\omega_{11}$ - $\Delta\omega_{13}$		$\Delta\omega_{10}$ – $\Delta\omega_{12}$		$\Delta\omega_{15}$ - $\Delta\omega_{3}$	
	M_p	T_s	M_p	T_s	M_p	T_s
AIT2FSMC-PSS	**1.697×10^{-3}**	**2.502 sec.**	**1.428×10^{-3}**	**2.423 sec.**	**1.219×10^{-3}**	**2.584 sec.**
AFSMC-PSS	4.792×10^{-3}	3.544 sec.	3.734×10^{-3}	3.147 sec.	5.183×10^{-3}	3.291 sec.
FSMC-PSS	8.851×10^{-3}	4.471 sec.	8.428×10^{-3}	4.112 sec.	8.834×10^{-3}	4.149 sec.
FPSS	10.41×10^{-3}	5.944 sec.	8.643×10^{-3}	7.098 sec.	10.78×10^{-3}	5.099 sec.
CPSS	14.06×10^{-3}	7.743 sec.	13.78×10^{-3}	8.242 sec.	13.32×10^{-3}	6.017 sec.

Again a comparison of PIs of MMPS is presented in Table-8 and Table-9 respectively. Small signal stability analysis is given in Table-8 whereas transient stability analysis is given in Table-9. Both small signal and transient stability analysis indicate the robust performance of the proposed AIT2FSMC-PSS with least values of its peak and settling characteristics.

A comparison of ITAE values and FD values of the proposed stabilizers are presented in bar chats as presented in Fig. 12 (a)-(c) and Fig. 13 (a)-(c) respectively. The least values of these indices indicate better stability performance of the stabilizers. The bar chats indicate that AIT2FSMC-PSS possesses minimum of ITAE and FD values to that of other stabilizers. It proves the improved stability performance of the proposed stabilizer.

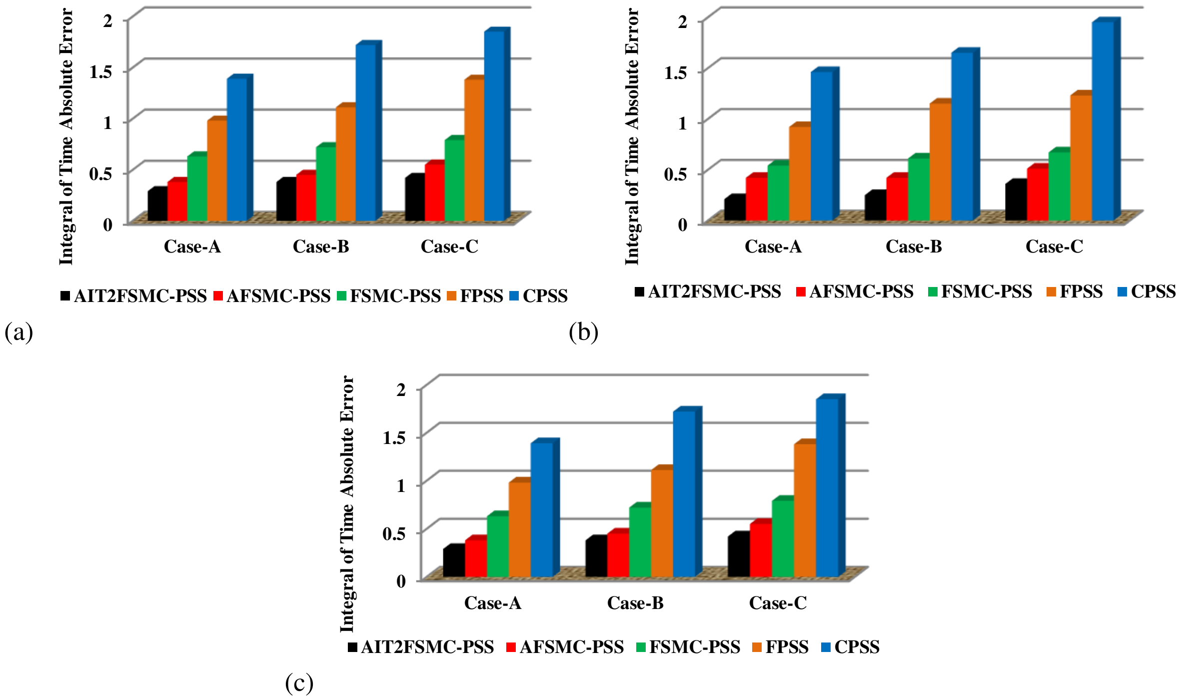

(a) (b) (c)

Fig. 12. ITAE values under (a) scenario-1 (b) scenario-2 (c) scenario-3.

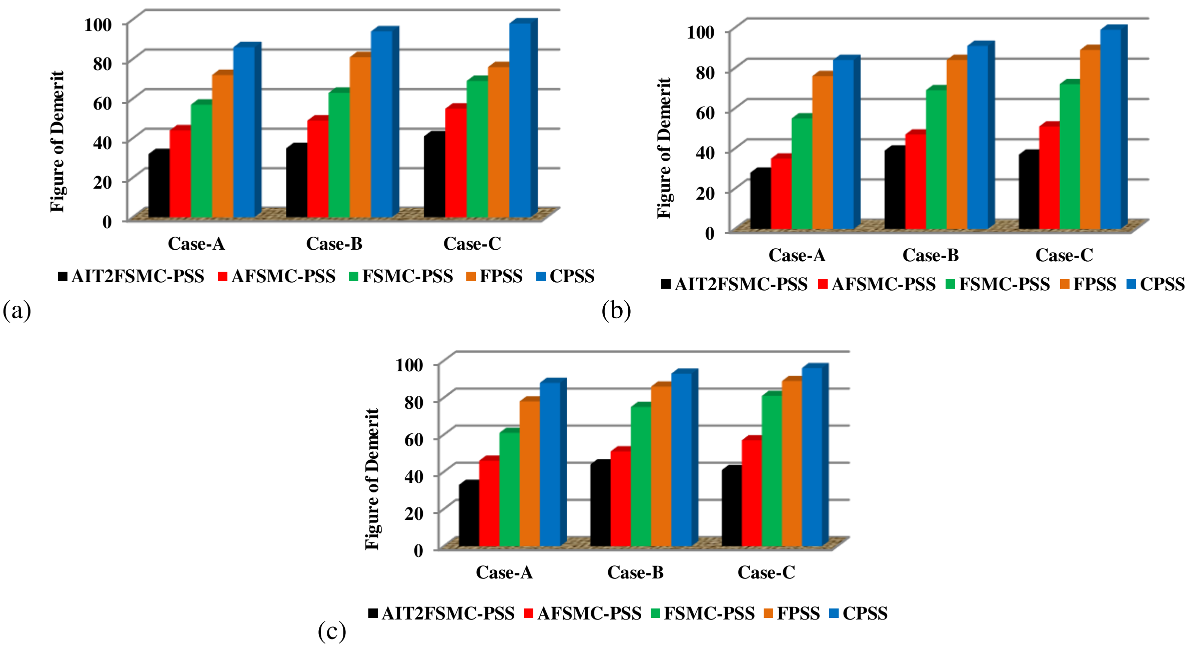

(a) (b) (c)

Fig. 13. Figure of demerit values (a) scenario-1 (b) scenario-2 (c) scenario-3.

4.5. Frequency Domain Analysis

This sub-section presents frequency stability analysis using Bode, root locus and Nyquist plot shown in Fig. 14 (a)-(d). From the linearized model, state matrices are derived and the above said plots are plotted. The root locus and its zoomed response are depicted in Fig. 14 (a)-(b). The plot clearly shows that the roots are more negative and located farther from the origin than that of other stabilizers. It shows the stable performance of the proposed stabilizer. Again, Bode plot in Fig. 14 (c) shows stable performance as both gain margin (GM) and phase margin (PM) are quite small in case on no control action which makes the system unstable. Whereas, GM and PM lies within infinity and -180^0 in case of the proposed AIT2FSMC-PSS than others The large values of GM and PM guarantee performance without loss of stability. Again, Nyquist plot shown in Fig. 14 (d) show stable performance of the proposed AIT2FSMC-PSS as the critical point (-1+j0) is encircled in counter clock wise direction which guarantees the stability.

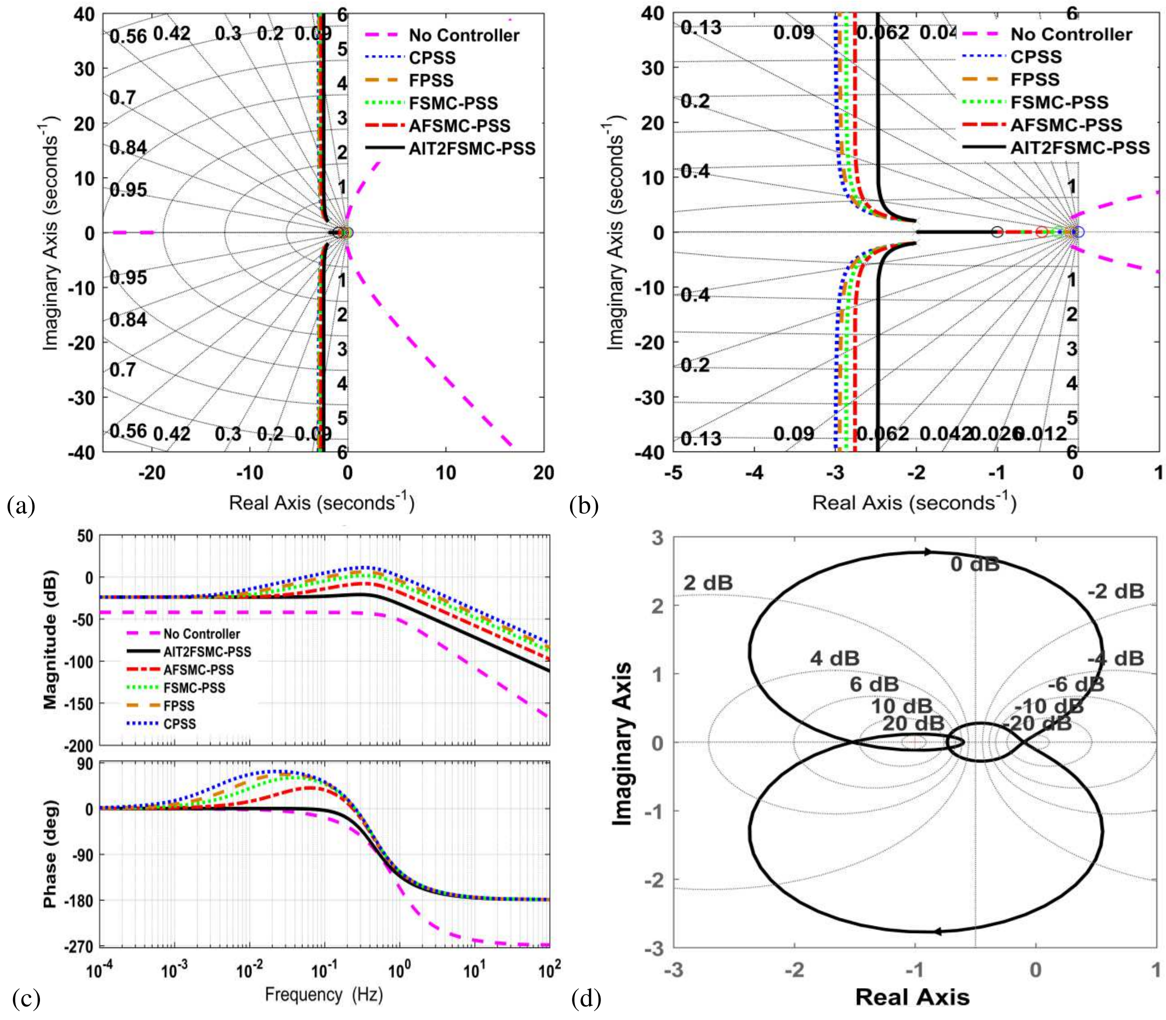

Fig. 14. Stability performance by means of (a) Root Locus (b) zoomed root locus (c) Bode plot (d) Nyquist plot.

5. Conclusion

A robust AIT2FSMC-PSS is presented for damping LFEOs in both SMIB and MMPS subjected to various uncertainties involving noises and external disturbances. A robust sliding surface is implemented to keep the system stable under disturbance conditions. A modified control law is presented to avoid chattering phenomenon select the parameters of IT2FLS. Lyapunov synthesis is adopted for the stability analysis and to assure the error asymptotically converges to zero even under uncertainties and external disturbances. Different uncertainties and fault disturbance scenarios are considered to authorize the efficacy of the proposed stabilizer. A comparison of PIs, ITAE, FD values along with Eigen values, damping ratios and oscillating frequencies are presented to support the simulations. Again, frequency domain stability analysis is also performed to ensure the stabilities of the proposed stabilizers. Both simulation and comparative analysis suggest the dominance of the proposed stabilizer in damping LFEOs in the power system than that of other stabilizers under different disturbance scenarios.

Appendix I

Parameters of SMIB system:

System Parameters: ω_b =314 rad/sec; S_b =160 MVA; V_b =15 kV.

Generator Parameters: X_d =1.7 p.u.; X_q =1.64 p.u.; X'_d =0.245 p.u.; T'_{d0} =5.9 sec.; H =2.37; D =0.

Parameters for Excitation System: K_A =50; T_A =0.045 sec.

Parameters for Transmission line: R_e =0.02 p.u.; X_e =0.5 p.u.

Rated Parameters: P =140 MW; Q =91.2 MVAR; V_t =12.4 kV$\angle$18.4^0; $V_{\inf}$ =15 kV$\angle$0^0; δ =49.16^0.

Parameters of CPSS:

K_{PSS} =50, T_w =10s, T_1 =1.99, T_2 =0.025s, T_3 =0.81, T_4 =0.004.

Declarations

Ethical approval

This article does not contain any studies with human participants or animals performed by any of the authors.

Funding Details

No funding is provided for the preparation of manuscript.

Conflict of interest

The authors declare that they have no conflict of interest.

Informed consent

The manuscript is submitted with the consent of all authors

6. References

[1] P. Kundur, Power system stability and control, McGraw-Hill, New York, 1994.
[2] P. M. Anderson, A. A. Fouad, Power system control and stability, 2nd ed., Wiley, 2003.
[3] S. R. Paital, P. K. Ray, A. Mohanty, Comprehensive review on enhancement of stability in multimachine power system with conventional and distributed generations, IET Renewable Power Generation, 12 (16), (2018) 1854-1863.
[4] Z. A. Obaid, L. M. Cipcigan, M. T. Muhssin, Power system oscillations and control: Classifications and PSSs' design methods: A review, Renewable and Sustainable Energy Reviews, 79 (2017) 839-849.
[5] F. P. deMello, C. A. Concordia, Concept of synchronous machine stability as affected by excitation control, IEEE Trans PAS, 103 (1969) 316–29.
[6] M. A. Hannan, N. N. Islam, A. Mohamed, A., et al., Artificial intelligent based damping controller optimization for the multi-machine power system: A review, IEEE Access, 6 (2018) 39574-39594.
[7] S. Chen, O. P. Malik, H-infinity optimization-based power-system stabilizer design, IEE Proceedings-Generation Transmission and Distribution, 142 (2) (1995) 179-184.
[8] M Kashki, M. A. Abido, Y. L. Abdel-Magid, Pole placement approach for robust optimum design of PSS and TCSC-based stabilizers using reinforcement learning automata, Electrical Engineering 91(7) (2010) 383-394.
[9] H. Werner, P. Korba, T. C. Yang, Robust tuning of power system stabilizers using LMI-techniques, IEEE Transactions on Control Systems Technology 11(1) (2003) 147-152.

[10] P. K. Ray, S. R. Paital, A. Mohanty, T. K. Panigrahi, M. Kumar, H. Dubey, Swarm and bacterial foraging based optimal power system stabilizer for stability improvement, In *IEEE Region 10 Conference (TENCON)*, 2016, pp. 1916-1920.

[11] L. Chaib, A. Choucha, S. Arif, Optimal design and tuning of novel fractional order PID power system stabilizer using a new metaheuristic Bat algorithm, *Ain Shams Engineering Journal 8*(2) (2017) 113-125.

[12] P.K. Ray, S.R. Paital, A. Mohanty, F. Y. Eddy, A. Krishnan, H. B. Gooi, and G. A. J. Amaratunga, 2018, May. Firefly algorithm scaled fractional order fuzzy PID based PSS for transient stability improvement. In *2018 19th International Carpathian Control Conference (ICCC)* (pp. 428-433). IEEE.

[13] H. Shayeghi, H. A. Shayanfar, A. Safari, R. Aghmasheh, A robust PSSs design using PSO in a multi-machine environment, *Energy Conversion and Management 51*(4) (2010) 696-702.

[14] D. Chitara, K. R. Niazi, A. Swarnkar, N. Gupta, Cuckoo Search Optimization Algorithm for Designing of a Multimachine Power System Stabilizer, *IEEE Transactions on Industry Applications* 54, (4) (2018) 3056-3065.

[15] E. S. Ali, Optimization of power system stabilizers using BAT search algorithm, *International Journal of Electrical Power & Energy Systems* 61 (2014) 683-690.

[16] S. M. Abd-Elazim, E. S. Ali, A hybrid particle swarm optimization and bacterial foraging for optimal power system stabilizers design, *International Journal of Electrical Power & Energy Systems* 46 (2016) 334-341.

[17] M. Singh, R. N. Patel, D. D. Neema, Robust tuning of excitation controller for stability enhancement using multi-objective metaheuristic Firefly algorithm, *Swarm and evolutionary computation* 44 (2019) 136-147.

[18] A. Hariri, O. P. Malik, A fuzzy logic based power system stabilizer with learning ability, *IEEE Transactions on Energy Conversion 11*(4) (1996) 721-727.

[19] D. K. Sambariya, R. Gupta, R. Prasad, Design of optimal input–output scaling factors based fuzzy PSS using bat algorithm, *Engineering Science and Technology, an International Journal* 19(2) (2016) 991-1002.

[20] S. R. Paital, P. K. Ray, A. Mohanty, November. Firefly-swarm optimized fuzzy adaptive PSS in power system for transient stability enhancement, In IEEE *Progress in Electromagnetics Research Symposium-Fall (PIERS-FALL), 2017,* pp. 1969-1976.

[21] T. T. Lie, A. M. Sharaf, An adaptive fuzzy logic power system stabilizer, *Electric power systems research 38*(1) (1996) 75-81.

[22] T. Hussein, M. S. Saad, A. L. Elshafei, A. Bahgat, Damping inter-area modes of oscillation using an adaptive fuzzy power system stabilizer, *Electr Pow Syst Res.* 80 (2010) 1428–36.

[23] S. R. Paital, P. K. Ray, S. R. Mohanty, S.R. and A. Mohanty, 2021. An adaptive fractional fuzzy sliding mode controlled PSS for transient stability improvement under different system uncertainties. *IET Smart Grid*, *4*(1), pp.61-75.

[24] S. R. Paital, P. K. Ray, A. Mohanty and G. Panda, 2021, March. Neuro-Fuzzy Sliding Mode Control based Wide Area Power System Stabilizer For Transient Stability Improvement. In *2020 3rd International Conference on Energy, Power and Environment: Towards Clean Energy Technologies* (pp. 1-6). IEEE.

[25] E. Nechadi, M. N. Harmas, A. Hamzaoui, N. Essounbouli, A new robust adaptive fuzzy sliding mode power system stabilizer, International Journal of Electrical Power & Energy Systems, 42(1) (2012) 1-7.

[26] K. Saoudi, M. N. Harmas, Enhanced design of an indirect adaptive fuzzy sliding mode power system stabilizer for multi-machine power systems, International Journal of Electrical Power & Energy Systems 54 (2014) 425-431.

[27] P. K. Ray, S. R. Paital, A. Mohanty, F. Y. Eddy, H. B. Gooi, A robust power system stabilizer for enhancement of stability in power system using adaptive fuzzy sliding mode control, Applied Soft Computing 73 (2018) 471-481.

[28] M. Farahani, S. Ganjefar, Intelligent power system stabilizer design using adaptive fuzzy sliding mode controller, Neurocomputing 226 (2017) 135-144.

[29] O. Castillo, P. Melin, A review on the design and optimization of interval type-2 fuzzy controllers, Applied Soft Computing 12(4) (2012) 1267-1278.

[30] H. Shokouhandeh, M. Jazaeri, An enhanced and auto-tuned power system stabilizer based on optimized interval type-2 fuzzy PID scheme, International Transactions on Electrical Energy Systems 28(1) (2018) 2469.

[31] D. K. Sambariya, R. Prasad, Design and small signal stability enhancement of power system using interval type-2 fuzzy PSS, Journal of Intelligent & Fuzzy Systems 30(1) (2016) 597-612.

[32] Z. Sun, N. Wang, D. Srinivasan, Y. Bi, Optimal tuning of type-2 fuzzy logic power system stabilizer based on differential evolution algorithm, International Journal of Electrical Power & Energy Systems 62 (2014) 19-28.
[33] P. K. Ray, S. R. Paital, A. Mohanty, Y. E. Foo, A. Krishnan, H. B. Gooi, G. A. Amaratunga, A hybrid firefly-swarm optimized fractional order interval type-2 fuzzy PID-PSS for transient stability improvement, IEEE Transactions on Industry Applications 55(6) (2019) 6486-6498.
[34] F. M. Adjeroud, F. Djahli, A. Mayouf, T.Devers, A coordinated genetic based type-2 fuzzy stabilizer for conventional and superconducting generators, Electric Power Systems Research 129 (2015) 51-61.
[35] T. M. R. Akbarzadeh, S. A. Hosseini, M. B. Naghibi-Sistani, Stable indirect adaptive interval type-2 fuzzy sliding-based control and synchronization of two different chaotic systems, Applied Soft Computing 55 (2017) 576-587.
[36] E. Nechadi, M. Harmas, Multi-machine power system stabilizer using type-2 adaptive fuzzy sliding mode controller, Eur J Adv Eng Technology 2(8) (2015) 1-8.
[37] R. Devarapalli, B. Bhattacharyya, N. K. Sinha and B. Dey, 2021. Amended GWO approach based multi-machine power system stability enhancement. *ISA transactions*, *109*, pp.152-174.
[38] J. M. Mendel, Type-2 fuzzy sets and systems: An overview, IEEE Comput. Intell. Mag. 2(1) (2007) 20–29.
[39] S. R. Paital, P. K. Ray and S. R. Mohanty, 2021. A robust dual interval type-2 fuzzy lead-lag based UPFC for stability enhancement using Harris Hawks Optimization. *ISA transactions*.
[40] Y. Hashemi, H. Shayeghi, M. Moradzadeh, Design of dual-dimensional controller based on multi-objective gravitational search optimization algorithm for amelioration of impact of oscillation in power generated by large-scale wind farms, Applied Soft Computing 53 (2017) 236-261.